Korean J. Chem. Eng., 34(5), 1456-1465 (2017)
DOI: 10.1007/s11814-017-0042-0

pISSN: 0256-1115
eISSN: 1975-7220

Investigation of hydrodynamic and mass transfer of mercaptan extraction in pulsed and non-pulsed packed columns

Pouria Amani*,†, Mohammad Amani, and Reza Hasanvandian***

*Department of Chemical Engineering, School of Engineering, University of Tehran, Tehran, Iran
**Mechanical and Energy Engineering Department, Shahid Beheshti University, Tehran, Iran
(*Received 10 December 2016 • accepted 14 February 2017*)

Abstract−We investigated the hydrodynamic behavior and mass transfer characteristics of a pilot-scale conventional packed bed extraction column of mercaptan removal from liquid propane. The extraction column was filled with pall rings structured packing where mercaptan was extracted from the continuous phase to the dispersed phase, accompanied by a chemical reaction in propane-mercaptan-caustic system. The pulsing was introduced into the column to enhance the mass transfer rate. Hydrodynamic parameters such as hold up, flooding velocity and mean drop size were studied together with the effect of chemical reaction on increasing mass transfer performance. Finally, the mass transfer and axial mixing coefficients were obtained from the optimization of data by ADM. It was found that at the pulsation intensity from 0.003 to 0.007 m/s, the maximum mass transfer and minimum axial mixing occurred and it can be concluded that pulsation improves the efficiency of mass transfer just at low intensities.

Keywords: Liquid-liquid Extraction, Mercaptan Removal, Pulsed Packed Column, Sulfrex Process, Axial Dispersion Model

INTRODUCTION

Solvent extraction is a very beneficial technique applied in diverse separation technologies such as chemical, petroleum, food, hydrometallurgy, and many other applications [1]. Extraction is a separation process with the aim of the purification of the feed along with the recovering of the compounds. In the design of an extraction column, the dimension of the column has to be specified in order to gain a desired mass transfer and maximum operating flow rates in all phases [2-4].

Optimal design of a solvent extraction column involves enhancing the column performance to achieve a higher rate of mass transfer as well as throughput of the column [5]. Van Dijck [6] proposed that the volumetric efficiency of a sieve-plate could be improved by either pulsing the liquids or reciprocating the plates. Pulsed columns are a type of liquid-liquid contactor in which the rate of the mass transfer has increased due to the hydraulic or pneumatic pulsation. The pulsed extraction column may be divided into several types, such as packed, sieve-plate, and disc and doughnuts. In particular, in packed columns the pulsation produces a wide dispersion of the liquids as well as eliminating the channeling, which leads to better contact between the dispersed and the continuous phases [2,3].

Structured packings have been increasingly used in the solvent extraction columns because packed columns provide higher efficiency as well as higher capacity in comparison with many other types of extractors [7-16]. Some industrial applications of solvent extraction with structured packings can be the removal of H_2S and mercaptans from LPG with MDEA and NAOH, respectively, the removal of flavor agent from an aqueous solution with alkane and removing ammonium sulfate from benzene-caprolactam with water [17]. The use of caustic sweetening for removing mercaptans sulfur from hydrocarbons is well known. Afshar et al. [18] focused on the extraction section of LPG sweetening process and studied the influence of extraction temperature, concentration, flow rate, and amount of caustic as alkaline solution on the extraction performance. Afshar and Hashemi [19] focused on the effect of temperature on mercaptans extraction and caustic regeneration and revealed that sodium mercaptide content in caustic along with sulfur impurities in product can be reduced due to good oxidation by optimization of temperature. Farshi and Rabiei [20] studied the kinetics of conversion in existing mercaptans in kerosene and analyzed impregnated activated carbon with powder of MEROX catalyst in laboratory scale. They observed poor impregnation efficiency due to pore diffusion resistance. They also proposed a kinetic model related to catalytic reaction for mercaptan conversion to disulfide in the presence of impregnated activated carbon with Merox catalyst. Koncsag and Barbulescu [21] conducted some experiments at laboratory and pilot scale structured packing columns to find a model for the calculation of the industrial scale column serving to the extraction of mercaptans. The equation for the hydrodynamic behavior of the column shows the dependency of the column capacity on the physical properties of the liquid-liquid system and the geometrical characteristics of the packing. Angelis [22] reviewed the mercaptan removal methods according to their molecular weight and content and revealed that large quantities of mercaptans are removed through extraction processes (Merox extraction, Merichem extraction), while small quantities are removed by scavengers.

†To whom correspondence should be addressed.
E-mail: pouria.amani@ut.ac.ir

Chantry et al. [23] exhibited 30% reduction of the required height of a packed column in case of pulse treatment. Mirzaie et al. [24] conducted an experimental investigation and CFD modeling of hydrodynamic parameters in a pulsed packed column. They revealed that the combination of computational fluid dynamics (CFD) and droplet population-balance model (DPBM) in the framework of Fluent can satisfactorily predict hydrodynamic parameters in a pulsed packed column. It is clear that pulsed columns have a beneficial merit over other mechanical contactors, especially in the case with high corrosive rate and radioactive systems [25]. Therefore, our objective was to investigate and compare packed and pulsed packed columns and discuss if a sensible enhancement in mass transfer occurs with introducing pulsation into the column.

To design or scale up an extraction column, it is essential to forecast the mass transfer behavior using a suitable mathematical model. In the literature, numerous mass transfer models including plug flow (PFM), axial dispersion (ADM), back flow and developed forward mixing model have been proposed [26-31]. Among these, PFM and ADM are the most recommended approaches for simulation and modeling of the extraction columns. ADM, originally introduced by Danckwerts [32], was a significant development in the modeling of mass transfer, because in this scheme all of the factors including the circulatory flow, small eddies, channeling and velocity profile are considered as a function of a particular parameter named axial dispersion coefficient (E). Morales et al. [33] and Sleicher [34] studied the deviation from ideal plug flow conditions caused by aforementioned factors. In particular, there are two typical ways to determine the axial dispersion coefficient of the dispersed and the continuous phases: it can be experimentally measured by using the tracer injection techniques [35,36], in which usually only one of the coefficients optimized, or it can be obtained from the experimental profile of solute concentration [37-39], where both coefficients will be optimized as well as $k_{oc}a$. Hufnagl et al. [40] by study the differential model in a Kuhni column, revealed that the hydrodynamic parameters show insignificant dynamic behavior of their own. Therefore, they suggested steady-state relationships for the determination of the parameters. Based on their results, the differential model adequately simulated the influence of disturbances, but no variation in the flow rates of the phases. Steiner et al. [41] studied the variation in hold-up, drop size distribution, and the solute concentration of the dispersed and the continuous phases along the column height in an extraction column filled with regular SMV Sulzer packing using differential contact model. They showed that using the constant average hydrodynamic parameters leads to the same results as in the case when the variation of these parameters is considered in terms of the position along the column. Weinstein et al. [42] developed a model to describe the hydrodynamics and mass transfer of a Kuhni column with toluene-water and acetone as the mass transfer agent. Their model involved the impact of the total balance equation in the dispersed phase. They evaluated two types of control systems: the conventional dispersion interface level control scheme by controlling the effluent flow rate of the continuous phase, and the model-based decentralized MIMO control scheme by controlling the feed flow rate of the continuous phase. The evaluation of the latter scheme showed the significant performance of the dynamic model. Xiaojin et al. [38] developed an improved dynamic combined model, with considering the impact of drop size distribution, in a coalescence-dispersion pulsed sieve-plate extraction column. The merit of this model is the one-dimension-search evaluation of the axial mixing, by using the two-point dynamic method to gain the stimulus-response curves. This model is one of the recommended models due to its accuracy, optimization with single parameter and simple boundary conditions.

We studied the hydrodynamics of a pilot-scale conventional packed bed extraction column of mercaptan removal from liquid propane and evaluated the variations of dispersed phase holdup, mean drop size and flooding points in the presence of pulsation. Moreover, by the use of ADM, the mass transfer behavior in a pulsed packed column was modeled and the overall mass transfer and axial mixing coefficients were studied at different operating conditions.

THEORETICAL FRAMEWORK

According to Mohanty [43], the available mathematical models proposed for liquid-liquid extraction can be classified into three basic groups: empiric, mixing cells and differential models, which can be subcategorized into pseudo-homogeneous dispersion and population balance dispersion models. In particular, the differential dispersion model demonstrates the physical behavior of a packed column. However, large amounts of data are required, which are very difficult to measure experimentally. Therefore, the simplification of the model and the reduction of mathematical complexity with preserving its applicability are essential tasks.

With respect to the column wall and internals which make fluids to flow in all directions, fluids have different characteristic velocities in the axial direction. However, in PFM, non-disturbed fluid without the departure from the ideal plug flow is assumed. Therefore, it is clear that PFM is far from reality. To address this problem, Danckwerts [32] proposed the axial dispersion coefficient, corresponding to the impacts of all the known and unknown parameters which lead to the departure from PFM. Thus, ADM is a realistic model that involves axial mixing and can be considered as a modification of PFM [44]. The assumptions made for the purpose of ADM are as follows:

- Mass transfer occurs from the surrounding liquid (continuous phase) to the drops (dispersed phase).
- The radial variation of velocity and concentration of the continuous and the dispersed phases are not considered. The mass transfer and in particular the concentration of solute highly affect the volumetric flow velocity.
- Drops are considered as rigid spheres and solute can be completely dissolved in the solvent.
- The axial dispersion coefficient of the dispersed phase is insignificant in comparison with that of the continuous phase, especially at high values of dispersed phase hold-up.
- The velocity of both phases is considered as nearly constant throughout the column, and using the average value for these parameters has been suggested.
- The volumetric mass transfer coefficient is considered as a constant value and is suggested to be averaged along the column.

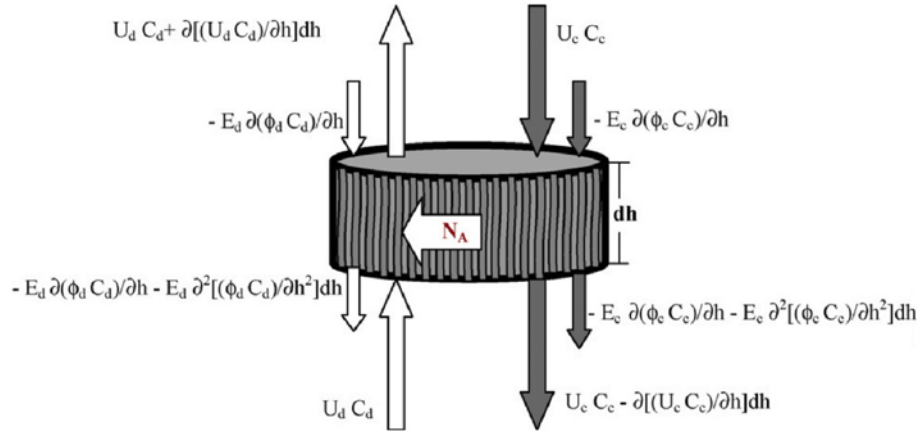

Fig. 1. Control volume for the differential dispersion model with mass transfer from the continuous to the disperse phase.

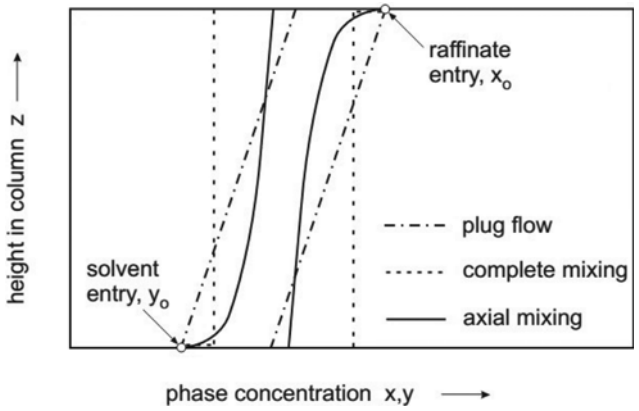

Fig. 2. The effect of axial mixing on the concentration profile.

- The reaction takes place in the aqueous phase.

Fig. 1 illustrates the control-volume approach to modeling mass transfer with the differential dispersion model. The larger and shorter arrows present the main flow and the axial mixing, respectively.

The influence of axial dispersion on the concentration profile along the column is presented in Fig. 2, which clearly shows that the presumption of non-disturbed flows with no deviation from ideal plug flows is not advisable since the internals and column wall make liquids stream in all directions. Accordingly, Danckwerts defined all influencing parameters in one parameter (E), namely, axial mixing coefficient which can be replaced on the diffusion coefficient in Fick's first law to determine the deviation from plug flow model.

According to Steiner and Hartland [45], the mass balance can be determined as follows:

$$N_A a_i = -K_{od} a_i (c_d - c_d^*) = -K_{oc} a_i (c_c^* - c_c) \quad (1)$$

The equilibrium concentration (c^*) of mercaptan in the hydrocarbon phase has been experimentally determined. The mass is transferred from the phase with higher chemical potential including concentration or partial pressure, to the areas of lower chemical potential until the equilibrium is reached [46].

A number of theories have been proposed to describe the mass transfer mechanism, including double stationary film theory, penetration theory, and surface renewal theory. The well-known double film theory can precisely describe the solvent extraction. In this model, mass transfer takes place within films by steady-state molecular diffusion. In the bulk of both phases, the concentration of the solute is considered uniform due to the high mixing [47]. But this theory does not represent mass transfer very reliably; in practice, the mass transfer film is not truly stagnant due to turbulence in the bulk phase. Highbie's penetration theory [48] considered the turbulent eddies penetrating the mass transfer film, thus renewing the fluid at the interface and hence enhancing mass transfer. Danckwerts [49] made a more sophisticated analysis of surface renewal.

Sometimes, chemical reaction occurs over the physical extraction process. Therefore, the extraction process can mostly be controlled either by the mass transfer or the chemical reaction, depending on the mass transfer rate or the chemical reaction rate, which has the lower value. Mass transfer with simultaneous chemical reaction is characterized using the *Hatta number* (Ha), which is the ratio of characteristic diffusion time to reaction time. If Ha>3, reaction is considered fast and proceeds mainly within the aqueous film near the liquid-liquid interface, whereas if Ha<0.3, the reactions are slow and occur mainly in the aqueous bulk. For a fast kinetics, the overall transformation rate is controlled by mass transfer. In Fig. 3(a), a particular case of fast reaction, the irreversible instanta-

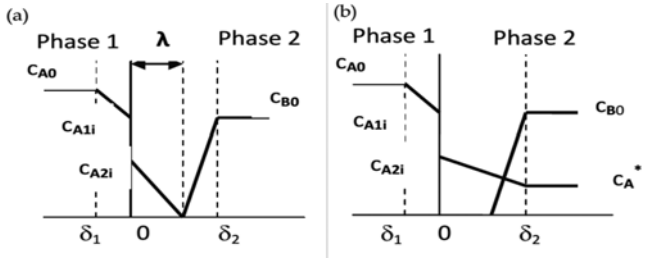

Fig. 3. Profiles of reactants concentration at the extraction with a chemical reaction: (a) instantaneous irreversible reaction taking place in phase film 2 and (b) slow reaction taking place in the film phase 2.

neous reaction is illustrated; in this case, both reactants diffuse to the reaction plane, where their concentrations equal zero. The term "instantaneous" is idealized since the reaction rate is always finite, but in this case, the mass transfer rate is much lower than the reaction rate, so the process is entirely controlled by the diffusion mechanism. On the other hand, the slow reaction can take place in the film, but more probably in the dispersed phase. In Fig. 3(b), the reaction takes place in the film phase 2. The process can be considered a physical diffusion of component A in the phase 2 film followed by reaction between A and B in the film of the phase 2. Unlike the fast reaction, part of component A remains unreacted and diffuses further in the phase 2, where its concentration is C_A^*. Fig. 3(b) illustrates the case when component B is completely consumed in the reaction, but there are more complicated cases when B is not consumed in the film phase 2, but diffuses further in the phase 1 and reaction could take place in one or both phases. Therefore, the rate of transfer for the extraction with slow reaction, depends both on the mass transfer coefficient and on the reaction rate constant.

The process is controlled by the slowest step: the mass transfer or the reaction. In this work, the reaction is considered fast and does not have any effect on controlling the rate. So, the overall mass transfer coefficient in the case of instant reaction is proportional to the coefficient for the physical extraction. It means that the coefficient at the extraction with instant chemical reaction depends on hydrodynamics to the same extent as that for physical extraction. In fact, chemical reaction is controlled only by mercaptan diffusion from organic phase, and the caustic concentration variation has insignificant influence on rate of reaction. Therefore, the reaction can be considered as a pseudo-first order. The acceleration of mass transfer across the liquid-liquid interface due to the chemical reaction in the interfacial region is often accounted for via so-called *enhancement factors* [50]. They can be obtained by fitting the experimental data or by simplified model assumptions. However, it is not possible to drive these factors properly from binary experiments and significant problems arise if reversible, parallel reactions take place [51]. For a fast liquid-liquid extraction, the volumetric extraction rate (R_2a) of a solute is given by Danckwert's model:

$$R_2a = ac_s\sqrt{D_{m,A}k_rc_2 + k_l^2} \tag{2}$$

Reactions in liquid-liquid systems can be classified from a kinetical point of view as slow, fast and instant. The equation describing the diffusion of the reactant simultaneously with the chemical reaction is:

$$D_A \cdot \nabla^2 C_A = u \cdot \nabla C_A + \frac{\partial C_A}{\partial t} + R_A \tag{3}$$

The term on the left-hand side of Eq. (3) represents the molecular diffusion of the component A through the film of phase 1, The terms on the right-hand side have the following meaning: the first one describes the transport by convection through the same film, the second one is the accumulation of A in the film, and the third represents the reaction rate. Eq. (3) can be simplified in the conditions of the double film theory, where the diffusion direction of A is perpendicular to the interface, eddies are inexistent in the film and component A does not accumulate in the film.

The resulting equations for both phases are:

$$\frac{\partial(\varphi_c C_c)}{\partial t} = -\frac{\partial(v_c C_c)}{\partial z} + E_c\left(\frac{\partial^2(\varphi_c C_c)}{\partial z^2}\right) - K_{oc}a(C_c - C_c^*) \tag{4}$$

$$\frac{\partial(\varphi_d C_d)}{\partial t} = +\frac{\partial(v_d C_d)}{\partial z} + E_d\left(\frac{\partial^2(\varphi_d C_d)}{\partial z^2}\right) + K_{oc}a(C_d - C_d^*) + R_A \tag{5}$$

In a steady state, there is no accumulation of mercaptan in any point of the system. This means that the rate of physical transfer process equals the consumption rate of mercaptan in reaction. The simplified model for both phases are:

$$E_c(1-\varphi_d)\frac{\partial^2 c_c}{\partial z^2} - v_c\frac{\partial c_c}{\partial z} - k_{oc}a(c_c - c_c^*) = 0 \tag{6}$$

$$E_d(1-\varphi_d)\frac{\partial^2 c_d}{\partial z^2} + v_d\frac{\partial c_d}{\partial z} + k_{oc}a(c_c - c_c^*) + R_A = 0 \tag{7}$$

Boundary conditions for Eqs. (6) and (7) are:

$$z = 0 \rightarrow -E_c\frac{dc_c}{dz} + \frac{Q_c}{S}c_c = \frac{Q_c}{S}c_{c,0},\ \frac{dc_d}{dz} = 0 \tag{8}$$

$$z = 1 \rightarrow \frac{dc_c}{dz} = 0,\ -E_d\frac{dc_d}{dz} + \frac{Q_d}{S}c_d = \frac{Q_d}{S}c_{d,0} \tag{9}$$

The arrangements of Eq. (6) and (7) have a complicated analytical solution, so the central finite difference method was employed to numerically solve the equation set. The values of $K_{oc}a$, E_c and E_d with respect to the solute concentration profile are optimized through the least square curve fitting method. In the present work, these calculations were done using a code developed on MATLAB Software.

EXTRACTION COLUMN DESCRIPTION AND METHODOLOGY

The extraction column of LPG treating unit of Iran's South Pars Gas Complex phases 9 and 10 has 1,250 mm diameter and 13,250 mm height. This unit is designed to process propane cut recovered in the NGL fractionation unit to extract the mercaptans prior to sending propane instead of sending to storage and export. The propane feed consists of mainly methyl, ethyl mercaptans, and COS with traces of H_2S. Maximum achievable mercaptans removal along with sulfur compounds from the propane cut is required due to commercial grade C_3 specification, which is needed to comply with basis of design and unit operating considerations prepared by Mehmandoost and Hejaz [52]. The sour LPG as fresh feed enters the unit and is cooled by the cooler before entering the extractor. The flow of continuous phase (propane) and the dispersed phase (NaOH solution) is counter-current in which propane enters the bottom of column. The continuous and dispersed phases have constant steady state flow. The mercaptan (propanethiol) is extracted with 12-15 wt% NaOH solution. The reaction of mercaptans with caustic soda to form sodium mercaptide is the main chemical reaction in the Sulfrex process extraction unit as follows:

$$RSH + \xleftrightarrow{NaOH\text{-}RSNa} + H_2O \tag{10}$$

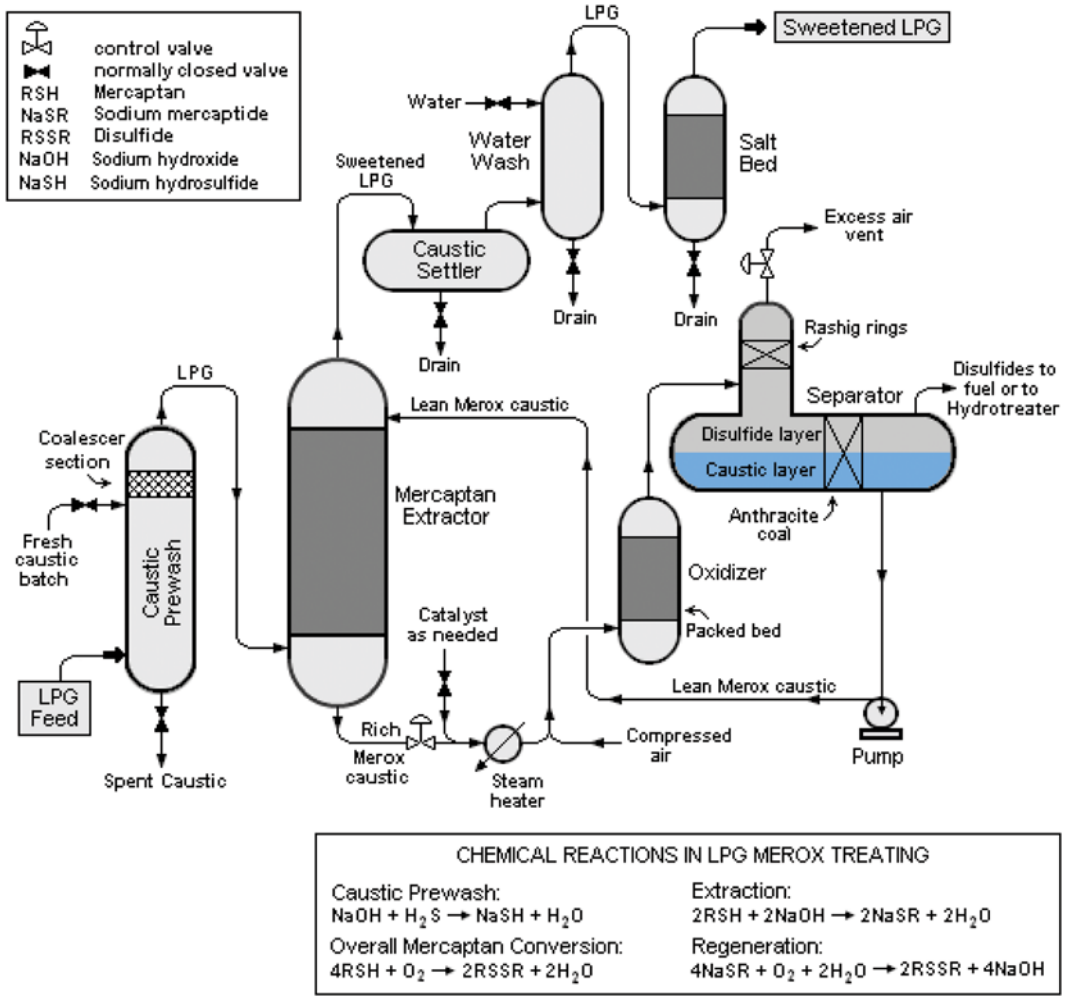

Fig. 4. Flow diagram of LPG Merox treating with its chemical reactions.

The propanethiol concentration in the propane feed and raffinate was measured by ASTM D1266, which were 560 ppm and 30 ppm, respectively. The propanethiol concentration in the extract (NaOH solution) was found by material balance. The plant flow diagram and the pall rings used are shown in Figs. 4 and 5. The raw feed and sweet product composition are presented in Tables 1 and 2.

Fig. 5. Column packing: Pall rings.

The pilot plant used in this study has a 125 mm diameter and 1,325 mm height. The column was filled with pall rings structured packing with the specific area of 350 m^2/m^3 and the void fraction of 95%. The packing bed was made of four structured packing elements with a total height of 1,200 mm. Compressed air is applied into the column for exerting pulsation along with a system com-

Table 1. Raw feed composition of LPG treatment unit

Composition	Propane cut
C_2	0.2%wt
C_3	99.1%wt
iC_4	0.4%wt
nC_4	0.1%wt
C_5^+	Trace
H_2S	Trace
COS	120 ppm
CH_3SH	558 ppm
C_2H_5SH	31 ppm
C_3^+ Mercaptans	Trace
Feed MW	44.3

Table 2. Product composition of LPG treatment unit

Composition	% vol	% wt
C_2	2.0 max	-
C_3	96.0 max	-
iC_4	2.5 max	-
nC_4	-	-
iC_5	-	-
nC_5	-	-
C_6^+	-	-
Sulfur content	-	0.008 max
H_2S	-	Negative

prise of a pneumatic and a temporizer control valve steered by a solenoid valve to generate rectangular wave pulsations with independent control of the negative and the positive semiwaves. The considered pulsation range for extraction experiments using symmetrical waves is up to 3.2 cm/s.

After meeting the steady state condition, we collected samples of the organic and the aqueous phases and holdup from six taps placed along the column. Moreover, by using photograph technique, the size of the organic phase drops was measured through four gauges placed along the column using a Nikon D5000 digital camera. To determine the size of the drops, the recorded photographs were analyzed by AutoCAD software. In each region, more than 500 drops were analyzed to guarantee the statistical significance of the determined Sauter mean drop diameter. The Sauter drop diameter was then measured as follows:

$$d_{32}=\frac{\sum n_i d_i^3}{\sum n_i d_i^2}, \tag{11}$$

where n_i is the number of drops of mean diameter and d_i is the measured droplet diameter. The mean diameter (d_{32}), is correlated with the holdup φ and the interfacial area a:

$$a=\frac{6\varphi}{d_{32}} \tag{12}$$

Most of the drops were assumed to be spherical due to the insignificant deviations from spherical shape for the operating conditions evaluated in this study. However, in some cases ellipsoidal shapes were observed, which were characterized through measuring their major axis (d_H), and their minor axis (d_L), representing the largest distance between two points on a drop and the largest length of a line, at an angle of 90° to the major axis. Accordingly, to measure the drop distortion, the drop diameter with an equivalent sphere was determined by Eq. (13) as follows:

$$d_i=\sqrt[3]{d_{H,i}^2 d_{L,i}}. \tag{13}$$

During measurements of drop sizes, each measurement was repeated three times and the average value was considered to guarantee the statistical significance of the determined variables. The uncertainty of this method was determined by taking a digital photo of the column content and measuring the dimensions of the packings on the photo. The size of the packings was then calculated based on each characteristic length and the results were compared with the known sizes.

RESULTS AND DISCUSSION

For measuring the solute concentration in the dispersed and the continuous phases along the column length, in each experiment at steady state condition, solute concentration in two phases at inlet, and outlet streams and seven sampling valves were measured by UV/vis spectrophotometer analyzer. The amount of mercaptan in dispersed phase at the top of column was zero, and it extracted mercaptans until the concentration in continuous phase decreased to 79 ppm at operating condition.

Because the reaction rate was fast, in the upper section of the column, the difference between the interfacial and bulk concentrations in both phases was very large and RSH was negligible in the dispersed phase. In this period of the extraction process, the extraction rate was controlled by the mass transfer rate in the continuous phase because NaOH in the dispersed phase was much more excessive. The bottom section of the column was controlled mainly by the mass transfer rate due to the presence of a fast reaction.

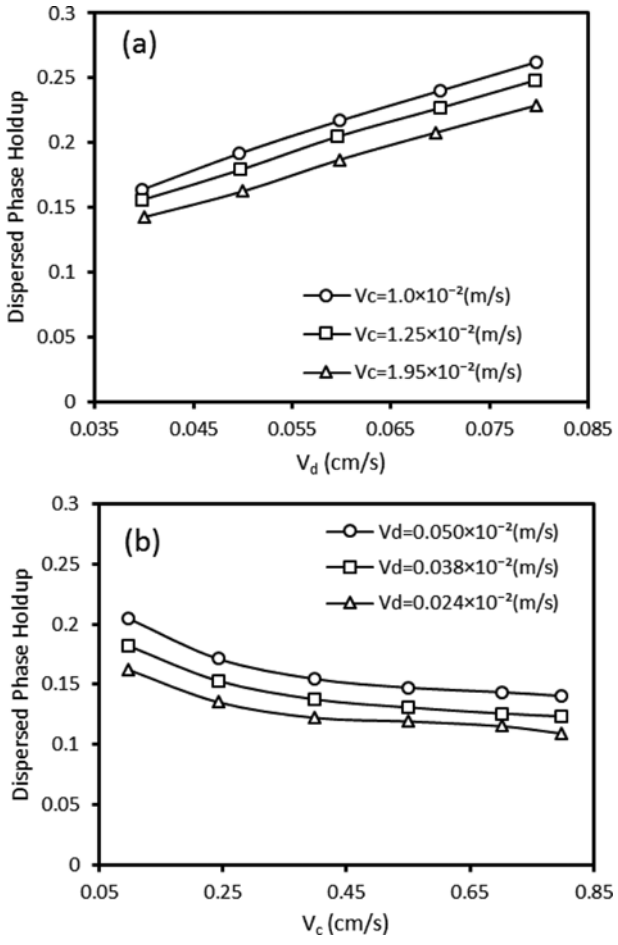

Fig. 6. Effect of the dispersed and continuous phase velocity on the dispersed phase hold-up under no pulsing conditions: (a) different dispersed phase velocities (b) different continuous phase velocities.

1. Effect of Pulsing Conditions on the Hydrodynamic Behavior of the Column

1-1. Hold-up

Fig. 6 shows the variation of the dispersed phase hold-up with changing the dispersed and continuous phase velocity under non-pulsing conditions. The continuous phase varied from 0.1×10^{-2} to 0.8×10^{-2} m/s, and the dispersed phase velocity had a range from 0.4×10^{-3} to 0.8×10^{-3} m/s. Fig. 6(a) shows that the dispersed phase hold-up increases when the dispersed phase velocity increments. On the other hand, Fig. 6(b) shows that there is a slightly downward trend with the continuous phase velocity. In fact, increasing the continuous phase velocity leads to the reduction of slip velocity between the phases. Therefore, the dispersed phase hold-up slowly decreases with an increase in the continuous phase velocity, and consequently the column becomes unstable at lower dispersed phase velocity.

The impact of pulsation intensity on the dispersed phase hold-up was investigated b yvarying the dispersed and continuous phase velocities, which is given in Fig. 7. It is achieved that the dispersed phase hold-up has relatively higher values at non-pulsing conditions (Af=0). With further increase in pulsation intensity, the dispersed phase hold-up experiences a decrease, followed by an upward trend at higher pulsation intensities due to an increase in drop breakage and consequently the formation of smaller drops. The minimum hold-up values, which results in the maximum throughput of the column, are found in Af=0.003-0.011 m/s for all dispersed and continuous phase velocity conditions.

Note that the minimum values of hold-up have also been reported for other pulsed extraction columns such as pulsed plate columns [53], disc and doughnut extraction columns [54] and a rotating impeller extraction column [55]. The explanation of this phenomenon can be referred to the different operating regimes introduced to characterize the hydrodynamic of the extraction columns. According to the literature, for a constant flow rate of the continuous and dispersed phases, there are three stable operating regimes: mixer-settler, dispersion and emulsion. When the pulsation intensity is low, the column operates in the mixer-settler regime. In this regime, because of the presence of a thick layer of the dispersed phase, hold-up is high. However, as the pulsation intensity is increased further, the large drops formed due to pulsations have insufficient residence time to collect through the column. Therefore, the dispersed phase hold-up declines with increasing the pulsation intensity, reaching a minimum value, corresponding to the transition from the mixer-settler regime to the dispersion regime. With further increase in pulsation intensity, drop size decreases and hold-up begins to increase due to an increase in the inertial and shear forces on drops, which leads to a rise in drop breakage.

Regarding the variation in the dispersed phase velocities, a higher dispersed phase velocity leads to a higher dispersed phase hold-up. Moreover, comparing Fig. 7(a) and Fig. 7(b) reveals the fact that the variation of the continuous-phase velocity does not influence the hold-up as much as the dispersed phase velocity at a constant pulsation intensity.

1-2. Mean Drop Diameter

The Sauter-mean diameter is a key variable in extraction column design due to its influence on the terminal rise velocity of

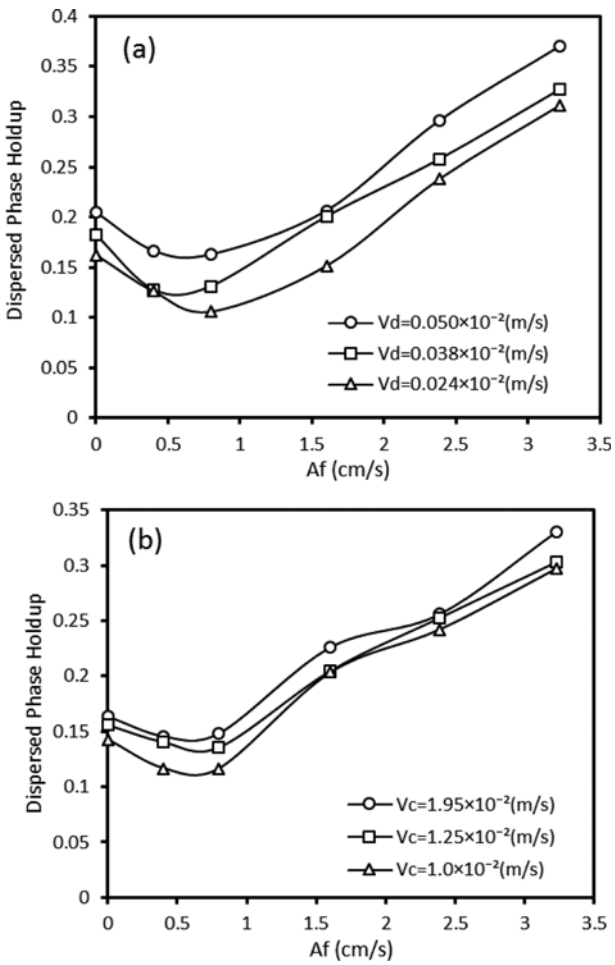

Fig. 7. Effect of pulsation on the dispersed phase hold-up under different phase velocities: (a) different dispersed phase velocities at constant continuous phase flow rate of 1.25×10^{-2} (b) different continuous phase velocities at constant dispersed phase flow rate of 0.038×10^{-3}.

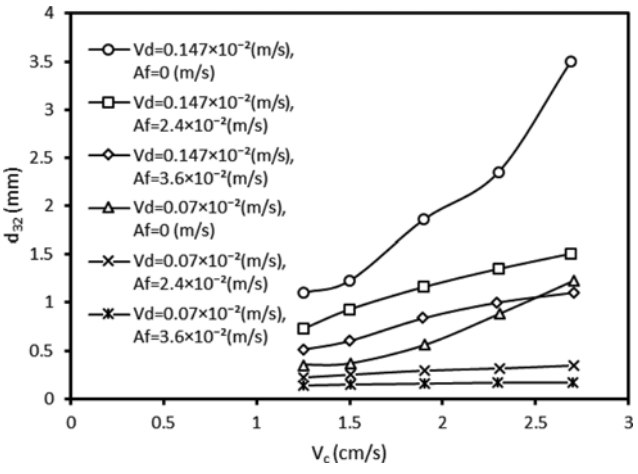

Fig. 8. Effect of the continuous phase velocity on the mean drop diameter at different pulsation intensity and the dispersed phase velocity.

drops, the dispersed phase hold-up, residence time of dispersed phase, axial dispersion and throughput. Moreover, the interfacial area available for mass transfer highly depends on drop size and plays an important role in the continuous and the dispersed phase mass transfer coefficients.

The effect of the operating parameters (pulsation intensity and the phase velocities) on the Sauter-mean diameter under different pulsing conditions is illustrated in Fig. 8. According the experimental observations, smaller drops are found at high pulsation intensity which is in accordance with the expectations because increasing the pulsation intensity results in higher dispersed phase drops breakage. With respect to the variation of dispersed phase velocity, higher dispersed phase velocity leads to the increase of mean drop size due to the higher coalescence rate. However, with incrementing the continuous phase velocity, the mean drop diameter slightly increases due to a rise in residence time and the reduction of slip velocity.

Fig. 8 clearly indicates that the impact of the phase velocities is different under different pulsing conditions. At non-pulsing conditions, the effects of the dispersed and the continuous phase velocities are much higher than that at the presence of the pulsation. The explanation can be the fact that the pulsation provides higher mixing and increasingly enhances the drop breakage, leading to much more convenient counter-current flow.

1-3. Flooding Points

The effect of pulsation intensity on flooding points at different flow ratio is shown in Fig. 9. Higher pulsation intensities, which produce smaller drops due to higher shear stress and more intense drop breakage, result in lower flooding velocities. Moreover, flooding velocity declines with an increase in the flow ratio of the dispersed phase to the continuous phase. In fact, at higher flow ratio, dispersed phase hold-up increases, and consequently the column reaches the flooding point at lower dispersed phase flow rate.

Furthermore, at non-pulsing conditions, the dispersed phase flooding velocity is relatively high. However, with further increase in pulsation intensity, the flooding velocity increases, reaching a maximum value, corresponding the higher maximum throughput. It is because at non-pulsing conditions, the structured packings act as a physical barrier in prohibiting counter-current flow of the two immiscible phases. Consequently, as pulsation is introduced into the column, shear forces on the drops increase and small drops are consequently produced. Therefore, hold-up of the column increases and the flooding velocity has higher values. However, after the flooding velocity reaches its maximum value, it experiences a decreasing trend with increase of pulsation intensity, due to an increase in drop breakage, and consequently the formation of smaller drops, which leads to an increase in hold-up. Therefore, it can be concluded that the maximum flooding velocities can be achieved at a certain range of pulsation intensities (Af=0.003-0.007 m/s), which is obtained for different flow ratios. The maximum value of flooding velocity with variation of pulsation intensity can also be referred to the operating regimes of the column. At lower pulsation intensity, the column performs in the mixer-settler regime. However, further increase of pulsation intensity leads to operating in the dispersion regime, followed by the emulsion regime. As discussed, there is an optimum range of pulsation intensity which leads to lower hold-up, higher value of flooding velocity and higher throughput.

2. Study of Overall Mass Transfer and Axial Dispersion Coefficients

The influence of the dispersed phase flow velocity and pulsation intensity on the overall mass transfer coefficient is shown in Fig. 10. $K_{oc}a$ incipiently increases with the increase of pulsation intensity, and after passing a maximum value it decreases. In fact, a higher pulsation intensity can greatly enhance the mass transfer driving force, and the available interfacial area will increase with the reduction of the dispersed phase drop diameter due to the pulsation. Therefore, $K_{oc}a$ increases. However, from Fig. 10, high pulsation intensity will aggravate the axial mixing, which results in the decrease of the mass transfer efficiency [44]. Therefore, it can

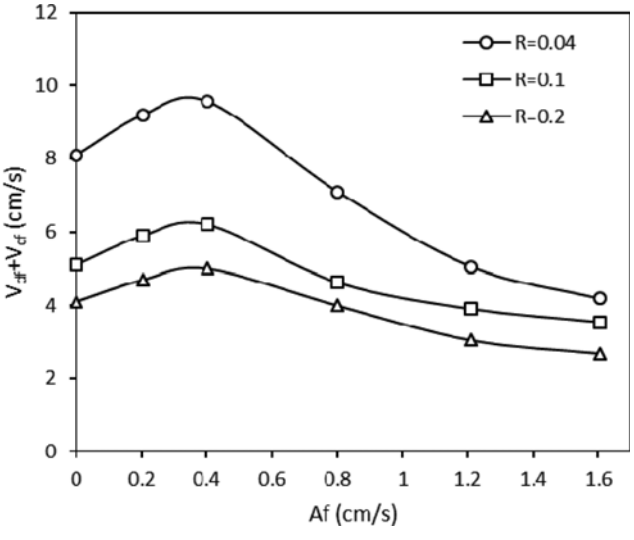

Fig. 9. Effect of the pulsation intensity on the flooding points in different flow ratio at constant continuous phase flow rate of 1.25×10^{-2}.

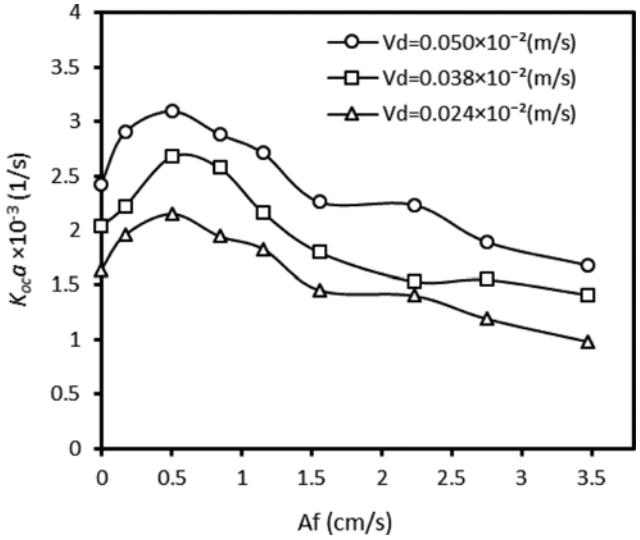

Fig. 10. Effect of pulsation intensity on the overall mass transfer coefficient at constant continuous phase flow rate of 1.25×10^{-2}.

Table 3. Axial dispersion coefficients obtained by AD model

Af (cm/s)	V_c (m/s)	V_d (m/s)	E_c (m^2/s)	E_d (m^2/s)
0.3	1.95×10^{-2}	0.24×10^{-2}	1.17×10^{-3}	1.18×10^{-4}
		0.38×10^{-2}	1.28×10^{-3}	1.20×10^{-4}
		0.50×10^{-2}	1.53×10^{-3}	1.20×10^{-4}
	1.00×10^{-2}	0.24×10^{-2}	8.71×10^{-4}	8.13×10^{-5}
		0.38×10^{-2}	9.21×10^{-4}	8.41×10^{-5}
		0.50×10^{-2}	1.15×10^{-3}	8.52×10^{-5}
0.8	1.95×10^{-2}	0.24×10^{-2}	1.22×10^{-3}	1.22×10^{-4}
		0.38×10^{-2}	1.27×10^{-3}	1.23×10^{-4}
		0.50×10^{-2}	1.41×10^{-3}	1.25×10^{-4}
	1.00×10^{-2}	0.24×10^{-2}	8.81×10^{-4}	8.54×10^{-5}
		0.38×10^{-2}	9.59×10^{-4}	8.85×10^{-5}
		0.50×10^{-2}	1.01×10^{-3}	9.03×10^{-5}

be concluded that in the range of pulsation intensity, the maximum value for the overall mass transfer coefficient can be attained (AF=0.003-0.007 m/s). However, in Safari et al. [44] and Jie and Weiyang [26] studies on water-acetone-toluene, water-acetone-butyl acetate and 30% tributyl phosphate kerosene-acetic acid-water systems, the maximum values for $K_{oc}a$ were obtained at about 0.008, 0.01 and 0.014 m/s of pulsation intensity.

Moreover, Fig. 10 shows that $K_{oc}a$ increases with an increase in the dispersed phase velocity. As illustrated in Figs. 7 and 8 the dispersed phase hold-up and mean drop size increases as the dispersed phase velocity increases. However, the dispersed phase hold-up in conjunction with the mean drop diameter determines the specific interfacial area by the formula $a=6\varphi/d_{32}$, where the hold-up growth can be considered six-times more effective than the mean drop diameter. Thus, the increase of $K_{oc}a$ by increasing the dispersed phase velocity can be referred to an increase in the interfacial area.

The axial dispersion coefficients of the dispersed and the continuous phases attained from data optimizing by ADM for some experiments are presented in Table 3. Accordingly, axial dispersion in the dispersed phase is considerably lower than that in the continuous phase. Moreover, at high pulsation intensity, axial mixing in each phase increases because of high population density of drops, the turbulence in the continuous phase, raising of the vortex of the continuous phase inside the column. Therefore, the axial dispersion of dispersed and continuous phase is strongly influenced by the pulsation intensity. From investigating the flow rates, the axial dispersion in each phase increases with incrementing the flow rate of dispersed and/or continuous phase flow rate.

Comparing the variation of mass transfer and axial mixing coefficients with pulsation intensity, there is a suitable region of pulsation intensity to maximize the mass transfer along with minimizing the axial mixing. The proportion of E_d/E_c along with some other parameters such as channeling and circulatory flows highly influence the drop size distribution, and according to Kumar and Hartland [56] and Safari et al. [44], the distribution of drops has a strong impact on the dispersed phase axial mixing in the column. Therefore, a large proportion of E_d/E_c causes the higher axial mixing in extraction column.

Table 3 shows that an increase of the dispersed phase velocity resulted in higher axial mixing coefficients. However, the effect of the dispersed phase velocity is higher on the E_d than E_c because higher dispersed phase velocity produces larger drops which rise faster because of higher upward buoyancy forces, leading to higher drop velocities, which increase the dispersed phase axial mixing.

CONCLUSION

We experimentally studied the hydrodynamic behavior and mass transfer characteristics of mercaptans extraction in a packed column under pulsing and non-pulsing conditions. The effects of operating parameters including pulsation intensity and the dispersed and continuous phase flow rate on the dispersed phase hold-up, mean drop diameter and flooding points were considered. Moreover, the overall mass transfer and the dispersed and the continuous phase axial mixing coefficients were obtained from optimization of data by ADM. The results show that the dispersed phase hold-up has relatively higher values at non-pulsing conditions. In the range of Af=0.003-0.011 m/s, the dispersed phase hold-up had a minimum value, which indicates the maximum allowable throughput of the column. Furthermore, introducing pulsation into the column leads to a reduction of drop sizes due to the higher drop breakage. The variation of flooding points under different pulsation intensities shows that in the range of Af=0.003-0.007 m/s, the column experiences its maximum available capacity.

According to the experimental observations, the $K_{oc}a$ incipiently increases with the enhancement of pulsation intensity, and after passing a maximum value it decreases. Axial dispersion coefficients in dispersed and continuous phases increase with introduction of pulsation intensity. However, because of the presence of more turbulent environment by applying pulsation, mass transfer performance will increase. The enhancement of mass transfer performance has a range and after passing a pulsation intensity region (Af=0.003-0.007 m/s), which corresponds to the maximum attainable throughput along with the highest mass transfer efficiency, it is followed by a reduction due to significant axial dispersion in both phases. Thus, it can be concluded that by introducing the pulsation into the packed column, the mass transfer and maximum capacity will increase due to a larger mass transfer area, until reaching a maximum and then followed by a reduction in extraction performance due to remarkable increase in axial dispersion.

NOMENCLATURE

Af : Pulsation intensity [m/s]
a : interfacial area per unit volume [m^2/m^3]
D : solute diffusion coefficient [m^2/s]
d_{32} : Sauter mean drop diameter [m]
E : axial dispersion coefficient [m^2/s]
H : column height [m]
K : mass transfer coefficient [kg/m^2 s]
V : characteristic velocity
S : column cross-section area [m^2]
Re : Reynolds Number $Re=\frac{\rho DV}{\mu}$

: Froude Number $Fr = \frac{V^2}{Dg}$

Greek Symbols

ρ : density [kg/m^3]
μ : viscosity [kg/m s]
ν : kinematic viscosity [m^2/s]
ε : porosity of packing [-]
φ : dispersed phase holdup [-]
Ω : $\frac{mV_d\rho_d}{V_c\rho_c}$ [-]

Subscripts

d : dispersed phase
c : continuous phase
f : flooding
o : overall based on (c or d)

REFERENCES

1. S. C. Lee and G. H. Hyun, *Korean J. Chem. Eng.*, **19**, 827 (2002).
2. G. H. Jeong and C. Kim, *Korean J. Chem. Eng.*, **1**, 111 (1984).
3. Y. K. Choi and C. Kim, *Korean J. Chem. Eng.*, **11**, 81 (1994).
4. S. Akhgar, J. Safdari, J. Towfighi, P. Amani and M. H. Mallah, *RSC Adv.*, **7**, 2288 (2017).
5. D. H. Han and W. H. Hong, *Korean J. Chem. Eng.*, **15**, 324 (1998).
6. W. J. D. Van Dijck, US Patent, 2,011,186 (1935).
7. M. Rahimi and M. Mohseni, *Korean J. Chem. Eng.*, **25**, 395 (2008).
8. J.-K. Moon, C.-H. Jung, E.-H. Lee and B.-C. Lee, *Korean J. Chem. Eng.*, **23**, 1023 (2006).
9. Y. J. Lee, H. Jeong, H. K. Park, K. Y. Park, T. W. Kang, J. Cho and D.-S. Kim, *Korean J. Chem. Eng.*, **33**, 2418 (2016).
10. T. Saha, S. Kumar and S. K. Bhaumik, *Korean J. Chem. Eng.*, **33**, 3337 (2016).
11. H. Jie, M.-L. Jia, C.-B. Tan and J.-S. Sun, *Korean J. Chem. Eng.*, **28**, 2190 (2011).
12. J. A. Khan, Y. Jamal, A. Shahid and B. O. Boulanger, *Korean J. Chem. Eng.*, **33**, 582 (2016).
13. S. Singha and U. Sarkar, *Korean J. Chem. Eng.*, **32**, 20 (2015).
14. S. A. Jafari and A. Jamali, *Korean J. Chem. Eng.*, **33**, 1296 (2016).
15. Y. Jia, D. Du, X. Zhang, X. Ding and O. Zhong, *Korean J. Chem. Eng.*, **30**, 1735 (2013).
16. L. Mateo-Vivaracho, J. Cacho and V. Ferreira, *J. Chromatogr. A*, **1185**, 9 (2008).
17. E. R. W. Rousseau, *Handbook of separation process technology*, John Wiley & Sons (2009).
18. A. S. Afshar, S. R. Hashemi, M. Miri and P. Setayeshi, *Pet. Sci. Technol.*, **31**, 2364 (2013).
19. A. S. Afshar and S. R. Hashemi, *World Acad. Sci. Eng. Technol.*, **79**, 56 (2011).
20. A. Farshi and Z. Rabiei, *Pet. Coal*, **47**, 49 (2005).
21. C. I. I. Koncsag and A. Barbulescu, *Chem. Eng. Process. Process Intensif.*, **47**, 1717 (2008).
22. A. de Angelis, *Appl. Catal. B Environ.*, **113-114**, 37 (2012).
23. W. A. Chantry, R. L. Von Berg and H. F. Wiegandt, *Ind. Eng. Chem.*, **47**, 1153 (1955).
24. M. Mirzaie, A. Sarrafi, H. H. Pour, A. Baghaie and M. Molaeinasab, *Solvent Extr. Ion Exch.*, **34**, 643 (2016).
25. J. M. P. Q. Delgado, *Heat Mass Transf.*, **42**, 279 (2006).
26. Y. Jie and F. Weiyang, *Can. J. Chem. Eng.*, **78**, 1040 (2000).
27. D. Sanpui, M. K. Singh and A. Khanna, *Korean J. Chem. Eng.*, **21**, 511 (2004).
28. G. Angelov and C. Gourdon, *Korean J. Chem. Eng.*, **32**, 37 (2015).
29. J.-O. Choo, Y.-K. Yeo, M.-K. Kim, K.-S. Kim and K.-S. Chang, *Korean J. Chem. Eng.*, **15**, 90 (1998).
30. B.-S. Chun, H.-G. Lee, J.-K. Cheon and G. Wilkinson, *Korean J. Chem. Eng.*, **13**, 234 (1996).
31. D. Sanpui and A. Khanna, *Korean J. Chem. Eng.*, **20**, 609 (2003).
32. P. V. Danckwerts, *Chem. Eng. Sci.*, **2**, 1 (1953).
33. C. Morales, H. Elman and A. Pérez, *Comput. Chem. Eng.*, **31**, 1694 (2007).
34. C. A. Sleicher, *AIChE J.*, **5**, 145 (1959).
35. G. U. Din, I. R. Chughtai, M. H. Inayat, I. H. Khan and N. K. Qazi, *Sep. Purif. Technol.*, **73**, 302 (2010).
36. G. U. Din, I. R. Chughtai, M. H. Inayat and I. H. Khan, *Appl. Radiat. Isot.*, **67**, 1248 (2009).
37. H. B. Li, G. S. Luo, W. Y. Fei and J. D. Wang, *Chem. Eng. J.*, **78**, 225 (2000).
38. X. Tang, G. Luo and J. Wang, *Chem. Eng. Sci.*, **59**, 4457 (2004).
39. X. Tang, G. Luo, H. Li and J. Wang, *Comput. Chem. Eng.*, **30**, 978 (2006).
40. H. Hufnagl, M. McIntyre and E. Blaß, *Chem. Eng. Technol.*, **14**, 301 (1991).
41. L. Steiner, H. Bertschmann and S. Hartland, *Chem. Eng. Res. Des.*, **73**, 542 (1995).
42. O. Weinstein, R. Semiat and D. R. Lewin, *Chem. Eng. Sci.*, **53**, 325 (1998).
43. S. Mohanty, *Rev. Chem. Eng.*, **16**, 199 (2000).
44. A. Safari, J. Safdari, H. Abolghasemi, M. Forughi and M. Moghaddam, *Chem. Eng. Res. Des.*, **90**, 193 (2012).
45. L. Steiner and S. Hartland, *Handb. Fluids Motion*, 1049 (1983).
46. R. E. Treybal, *Mass-transfer operations*, New York (1981).
47. W. L. McCabe, J. C. Smith and P. Harriott, *Unit operations of chemical engineering*, New York, McGraw-Hill (1993).
48. R. Higbie, *Trans. Am. Inst. Chem. Eng.*, **35**, 36 (1935).
49. P. V. Danckwerts, *Ind. Eng. Chem.*, **43**, 1460 (1951).
50. D. W. van Krevelen and C. J. van Hooren, *Recl. des Trav. Chim. des Pays-Bas*, **67**, 587 (2010).
51. Z. O. Andrzej Gorak, *Distillation: Equipment and Processes*, Academic Press (2014).
52. S. Mehmandoost and P. Hejaz, Propane treatment unit, operating manual. Basis of design and unit operating considerations. Iran South Gas Field: Phases 9 & 10. Assaloyeh, Iran: Pars Oil and Gas Company (2005).
53. A. Prabhakar, G. Sriniketan and Y. B. G. Varma, *Can. J. Chem. Eng.*, **66**, 232 (1988).
54. Y. Wang, K. A. Mumford, K. H. Smith, Z. Li and G. W. Stevens, *Ind. Eng. Chem. Res.*, **55**, 714 (2016).
55. Y. K. Lee, D. P. Ju and C. Kim, *Korean J. Chem. Eng.*, **8**, 80 (1991).
56. A. Kumar and S. Hartland, *Ind. Eng. Chem. Res.*, **38**, 1040 (1999).